Supporting Information

High volatility of superbase-derived eutectic solvents used for CO_2 capture

Yu Chen[*,a], Xiaohong Hu[a], Wenjun Chen[b], Chong Liu[a], Kepan Qiao[a], Meijing Zhu[a], Yanyan Lou[a], Tiancheng Mu[*,b]

[a] Department of Chemistry and Material Science, Langfang Normal University, Langfang 065000, Hebei, China

[b] Department of Chemistry, Renmin University of China, Beijing 100872, China

[*] Yu Chen, E-mail: yuchen@iccas.ac.cn; Phone: +86-316-2188211; Fax: +86-316-2112462.

[*] Tiancheng Mu, E-mail: tcmu@ruc.edu.cn; Phone: +86-10-62514925; Fax: +86-10-62516444.

Contents

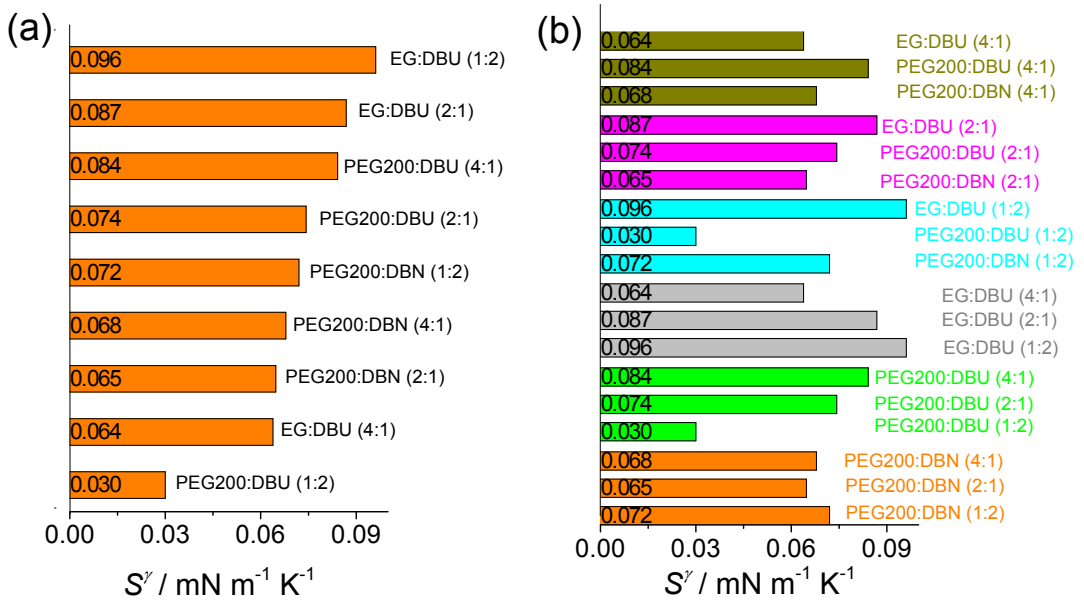

Figure S1. Entropy of surface formation (S^{γ}) of superbase-derived ESs in the order from the highest at the top to the lowest at the bottom (a) and the effect of mol ratio/components (b).

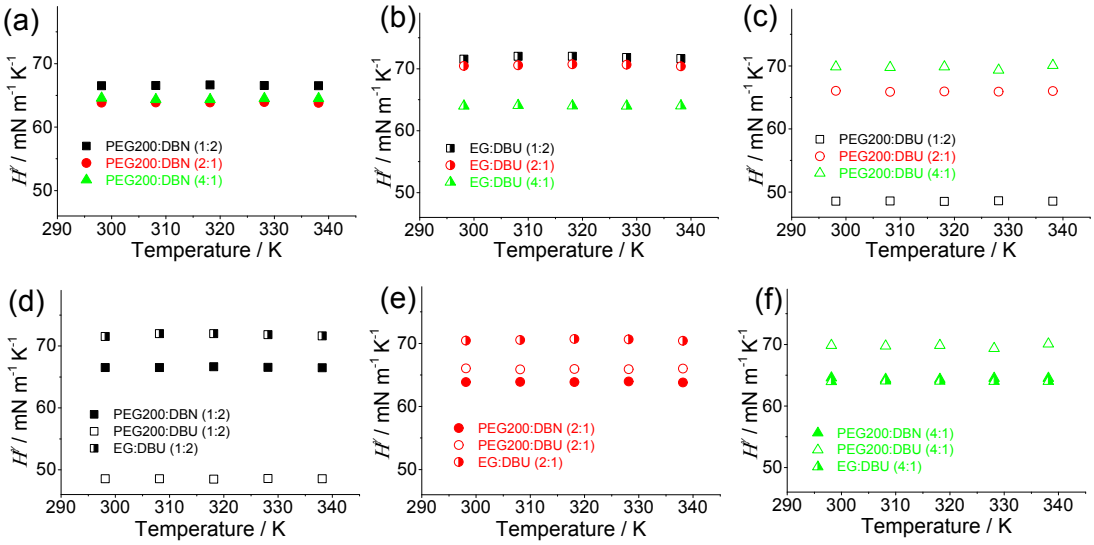

Figure S2. Effect of temperature on enthalpy of surface formation (H^{γ}) of superbase-derived ESs. PEG200:DBN (a), EG:DBU (b), PEG200:DBU (c) varying in mole ratio, 1:2 (d), 2:1 (e) and 4:1 mole ratio (f) varying in components.

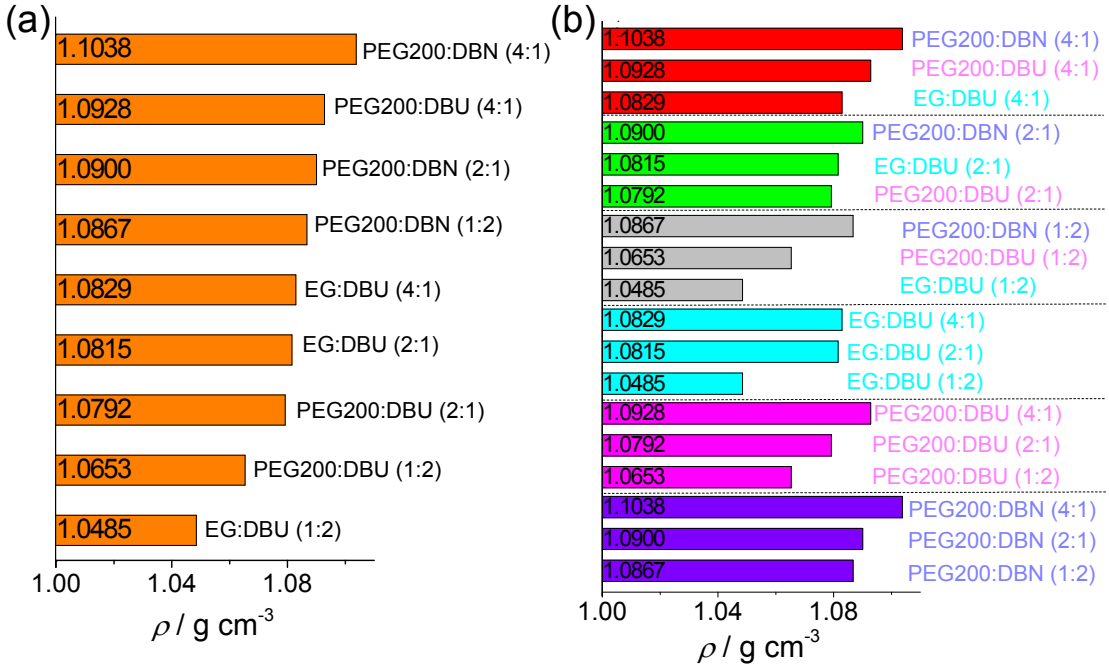

Figure S3. Density of superbase-derived ESs at 25 °C in the order from the highest at the top to the lowest at the bottom (a) and the effect of mol ratio/components (b).

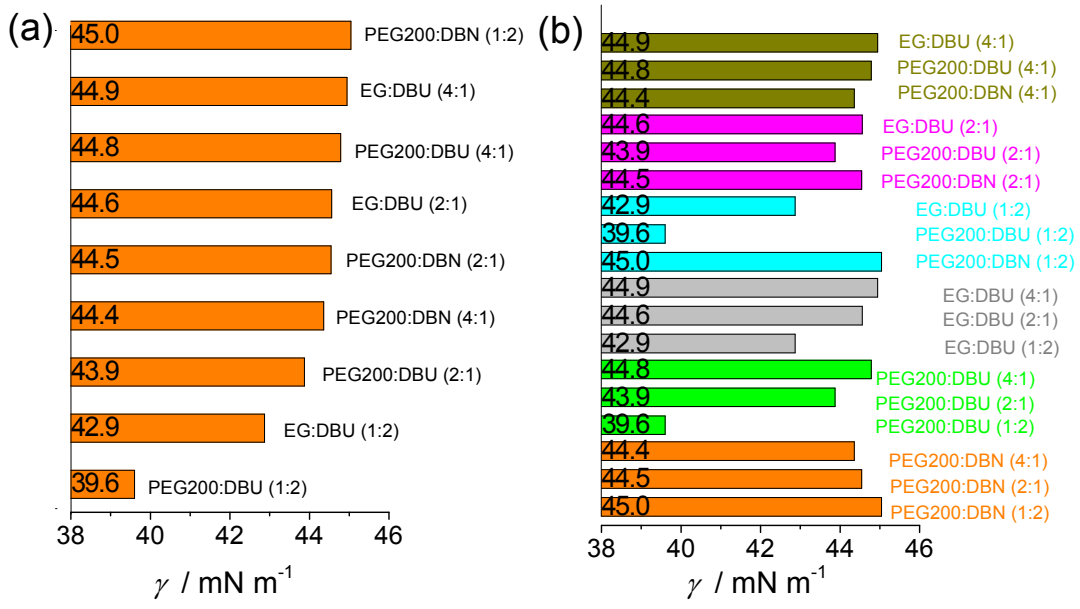

Figure S4. Surface tension of superbase-derived ESs at 25 °C in the order from the highest at the top to the lowest at the bottom (a) and the effect of mol ratio/components (b).

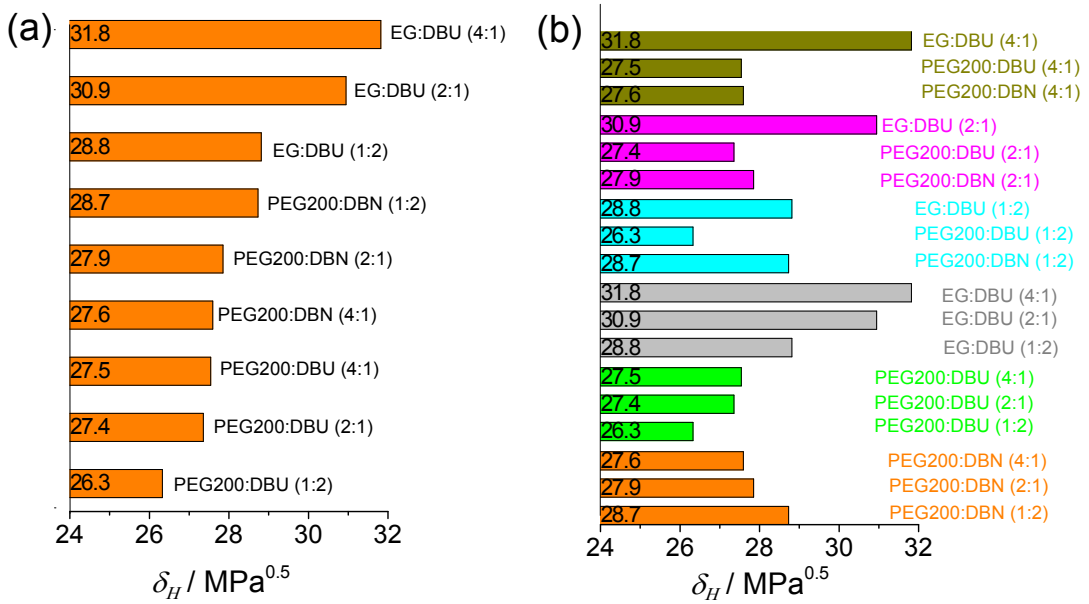

Figure S5. Solubility parameter of superbase-derived ESs at 25 °C in the order from the highest at the top to the lowest at the bottom (a) and the effect of mol ratio/components (b).

Table S1. Comparison of empirical constant (K) and critical temperature (T_c) for superbase-derived ESs varying in mole ratio and components.

Superbase-derived ESs	K / J K^{-1}	T_c / K
PEG200:DBN (1:2)	2.8E-07	774
PEG200:DBN (2:1)	2.7E-07	836
PEG200:DBN (4:1)	3.0E-07	802
PEG200:DBU (1:2)	1.5E-07	1119
PEG200:DBU (2:1)	3.2E-07	766
PEG200:DBU (4:1)	3.6E-07	729
EG:DBU (1:2)	2.9E-07	677
EG:DBU (2:1)	2.3E-07	715
EG:DBU (4:1)	1.6E-07	835
PEG200:DBN (1:2)	2.8E-07	774
PEG200:DBU (1:2)	1.5E-07	1119
EG:DBU (1:2)	2.9E-07	677
PEG200:DBN (2:1)	2.7E-07	836
PEG200:DBU (2:1)	3.2E-07	766
EG:DBU (2:1)	2.3E-07	715
PEG200:DBN (4:1)	3.0E-07	802
PEG200:DBU (4:1)	3.6E-07	729
EG:DBU (4:1)	1.6E-07	835

Table S2. Comparison of vaporization enthalpy and vapor pressure of representative superbase-derived ESs, ionic liquids and common organic solvents investigated at ca. 298.15 K.

Categories	Name	$\Delta_l^g H_m^0$ / kJ mol^{-1}	Reference	Name	Vapor pressure / Pa	Reference
ESs	PEG200:DBU (4:1)	134.7	this work	PEG200:DBU (4:1)	—	this work
ESs	PEG200:DBU (2:1)	130.1	this work	PEG200:DBU (2:1)	—	this work
ESs	PEG200:DBN (4:1)	130.0	this work	PEG200:DBN (4:1)	—	this work
ESs	PEG200:DBN (2:1)	126.8	this work	PEG200:DBN (2:1)	—	this work
ESs	PEG200:DBN (1:2)	116.0	this work	PEG200:DBN (1:2)	—	this work
ESs	PEG200:DBU (1:2)	111.9	this work	PEG200:DBU (1:2)	—	this work
ESs	EG:DBU (1:2)	99.2	this work	EG:DBU (1:2)	—	this work
ESs	EG:DBU (2:1)	84.1	this work	EG:DBU (2:1)	—	this work
ESs	EG:DBU (4:1)	77.4	this work	EG:DBU (4:1)	154.5	this work
organic solvents	n-hexadecane	81.4	[1]	propylene carbonate	8.5	[2]
organic solvents	n-dodecane	61.3	[1]	1-methylbenzimidazole	ca. 0.20	[3]
organic solvents	dimethylsulfoxide	52.9	[4]	1-methylbenzimidazole	ca. 1.15	[3]
organic solvents	dimethylformamide	49.2	[5]	1-ethylbenzimidazole	ca. 2.73	[3]
organic solvents	water	43.98	[6]	1-propylbenzimidazole	ca. 1.66	[3]
organic solvents	ethanol	42.32	[6]	1-butylbenzimidazole	ca. 0.78	[3]
organic solvents	methanol	37.43	[6]	1-pentylbenzimidazole	ca. 0.28	[3]
organic solvents	benzene	33.9	[1]	acetonitrile	11839	[7]
organic solvents	acetone	30.90	[1]	triethylamine	7599	[7]
organic solvents	n-hexane	31.5	[1]	N-methylpyrrolidone	44	[7]
organic solvents	n-pentane	26.7	[1]	dimethylsulfoxide	80	[7]
ionic liquids	$[C_1C_1IM][Glu]$	238.8	[8]	$[C_2C_1IM][NTf_2]^a$	1.05E-9	[9]
ionic liquids	$[C_6C_1IM][Glu]$	189.8	[8]	$[C_4C_1IM][NTf_2]^a$	8.37E-10	[9]
ionic liquids	$[H_2N\text{-}C_2C_1IM][PF_6]$	165.6	[10]	$[C_6C_1IM][NTf_2]^a$	4.67E-10	[9]
ionic liquids	$[H_2N\text{-}C_6C_1IM][PF_6]$	156.4	[10]	$[C_8C_1IM][NTf_2]^a$	7.98E-11	[9]
ionic liquids	$[C_1C_1IM][DMP]$	147.02	[6]	$[C_4C_1IM][NTf_2]^a$	2.72	[11]
ionic liquids	$[C_4C_2IM][DEP]$	133.72	[6]	ethyl ammonium nitrate	< 0.5	[2]
ionic liquids	$[C_2C_1IM][PF_3(CF_2CF_3)_3]$	157.8	[12]	$[C_6C_1IM][Thr]$	4.05E-6	[13]
ionic liquids	$[C_6C_1IM][PF_3(CF_2CF_3)_3]$	163.1	[12]	$[C_3C_1IM][Ac]^a$	1.73E-4	[14]
ionic liquids	[tmgH][L]	108.0	[15]			
ionic liquids	$[C_4C_1IM][NTf_2]$	134.6	[16]			
ionic liquids	$[C_8C_1IM][NTf_2]$	149.0	[16]			
ionic liquids	$[C_2C_1IM][B(CN)_4]$	130.9	[17]			
ionic liquids	$[C_2C_1IM][CF_3SO_3]$	132.8	[17]			
ionic liquids	$[C_1C_1IM][DMPO_4]$	111.3	[18]			
ionic liquids	$[C_2C_1IM][C_8SO_4]$	172.0	[19]			
ionic liquids	$[C_2C_1IM][FAP]$	125.8	[19]			
ionic liquids	[DBUH][nPrCOO]	190.5	[20]			
ionic liquids	$[C_2Py][Ntf_4]$	131.4	[21]			
ionic liquids	$[C_8C_8IM][Br]$	181.4	[22]			

[a] vapor pressure of these ionic liquids is derived from mathematical fitted Antoine model.

Table S3. Evaporation rate *dm/dt*, molecular weight *M*, *v* and vapor pressure *p* of EG at different temperature *T*.

T / °C	*T* / K	*dm/dt* / g min^{-1}	*M* / g mol^{-1}	*v* / g$^{0.5}$ min^{-1} mol$^{0.5}$ K$^{0.5}$	*p* / Pa
45	343.15	-9.48E-05	62.068	-2.2E-04	370.9
55	353.15	-1.70E-04	62.068	-4.1E-04	698.7
65	363.15	-2.24E-04	62.068	-5.4E-04	1265.7
75	373.15	-3.62E-04	62.068	-8.9E-04	2212.5
85	383.15	-5.75E-04	62.068	-0.0014	3743.7
95	393.15	-8.85E-04	62.068	-0.0022	6148.6

These data are extracted from the reference.[23]

Table S4. Mass loss of EG:DBU (4:1) at 1 h as the short-term volatility and at 20 h as the long-term volatility as a function of temperature.

T / °C	*T* / K	*Mass loss at 1 h* / %	*Mass loss at 20 h* / %
25	298.15	5.0	43.5
35	308.15	7.8	64.3
45	318.15	20.7	94.6
55	328.15	42.7	98.5
65	338.15	64.4	98.8

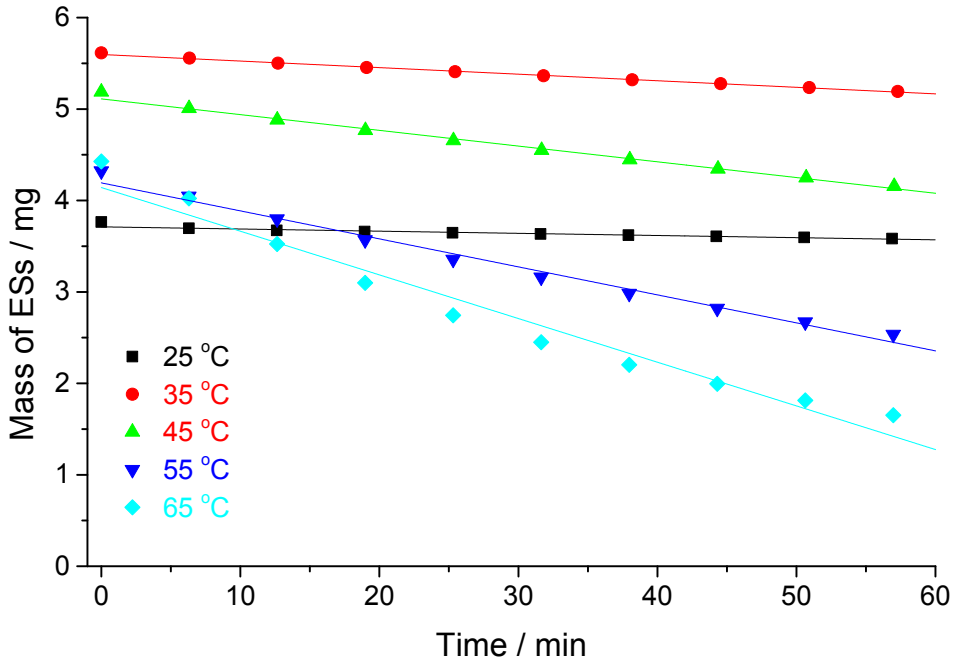

Figure S6. Mass of EG:DBU (4:1) as a function of time at 25 °C to 65 °C in the interval of 10 °C by TGA in the first 60 min (isothermal mode, nitrogen gas, platinum pan, skipped 100 points). These lines are the linear fitted lines for the purpose of obtaining *dm/dt*.

Table S5. Evaporation rate *dm/dt* of EG:DBU (4:1) as a function of temperature and the corresponding linearly fitted equation.

T / °C	T / K	Linearly fitted equation	R^2	dm/dt / g min^{-1}
25	298.15	m = -0.00237 t + 3.71171	0.9515	-0.00237
35	308.15	m = -0.00718 t + 5.59660	0.9978	-0.00718
45	318.15	m = -0.01720 t + 5.11105	0.9947	-0.01720
55	328.15	m = -0.03062 t + 4.19248	0.9877	-0.03062
65	338.15	m = -0.04776 t + 4.14163	0.962	-0.04776

Table S6. Vapor pressure of EG:DBU (4:1) as a function of temperature.[a]

T / °C	T / K	M / g mol^{-1}	k / Pa min g$^{-0.5}$ mol$^{-0.5}$ K$^{0.5}$	dm/dt / g min^{-1}	p / *Pa*
25	298.15	80.104	-2.66E6	-0.00237	154.5
35	308.15	80.104	-2.66E6	-0.00718	157.1
45	318.15	80.104	-2.66E6	-0.01720	159.6
55	328.15	80.104	-2.66E6	-0.03062	162.1
65	338.15	80.104	-2.66E6	-0.04776	164.6

[a] molecular weight of EG:DBU(4:1) is derived by averaging the molecular weight of EG and DBU with the mol ratio of 4:1.

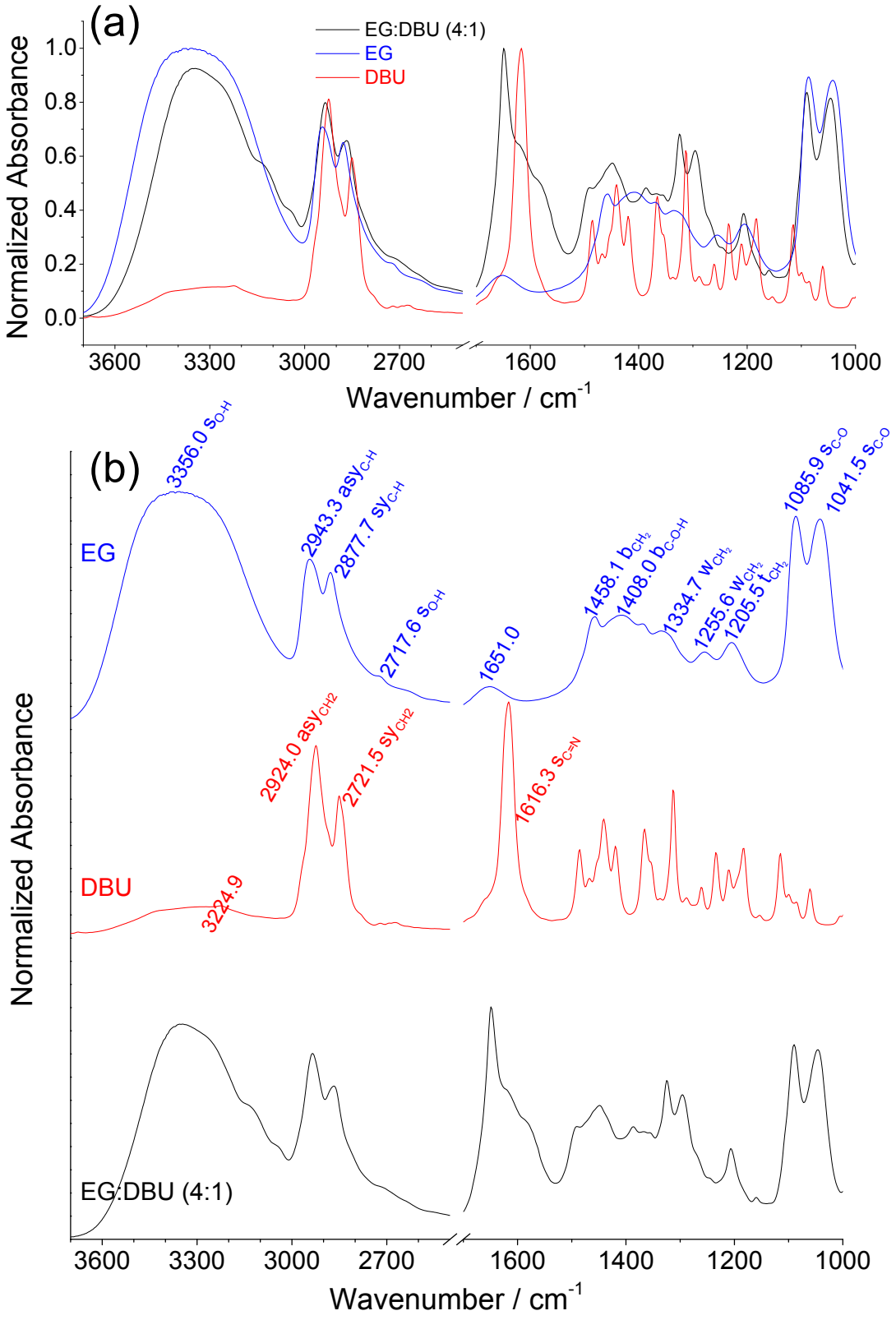

Figure S7. IR spectra of EG, DBU and EG:DBU (4:1) with converged comparison (a) and separately assignment (b).

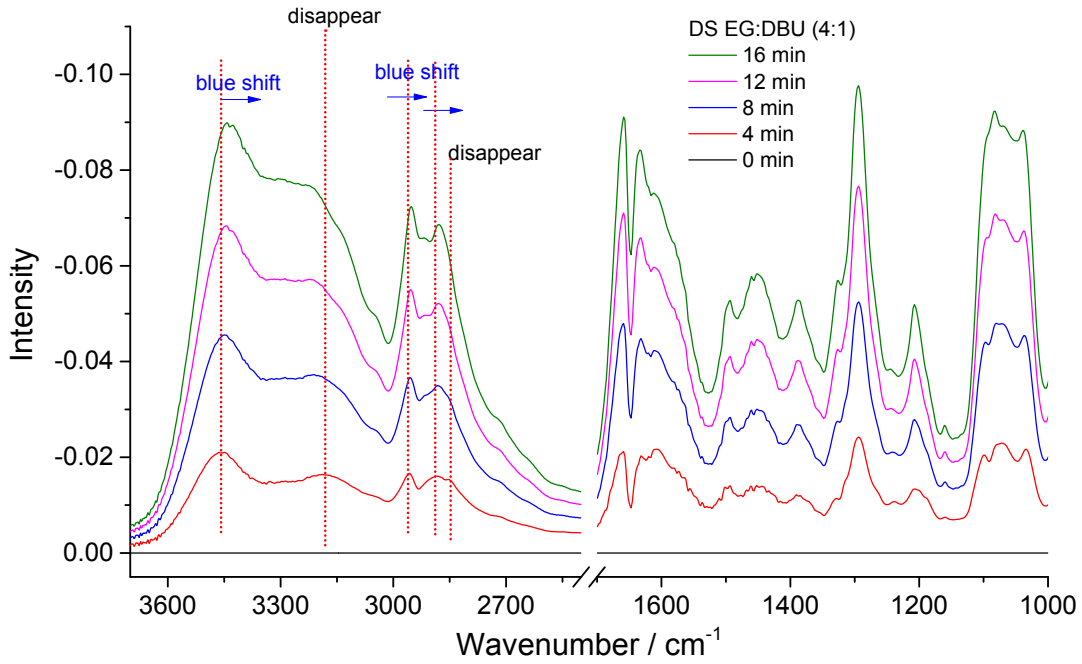

Figure S8. IR difference spectra (DS) of EG:DBU (4:1) in the first 16 min.

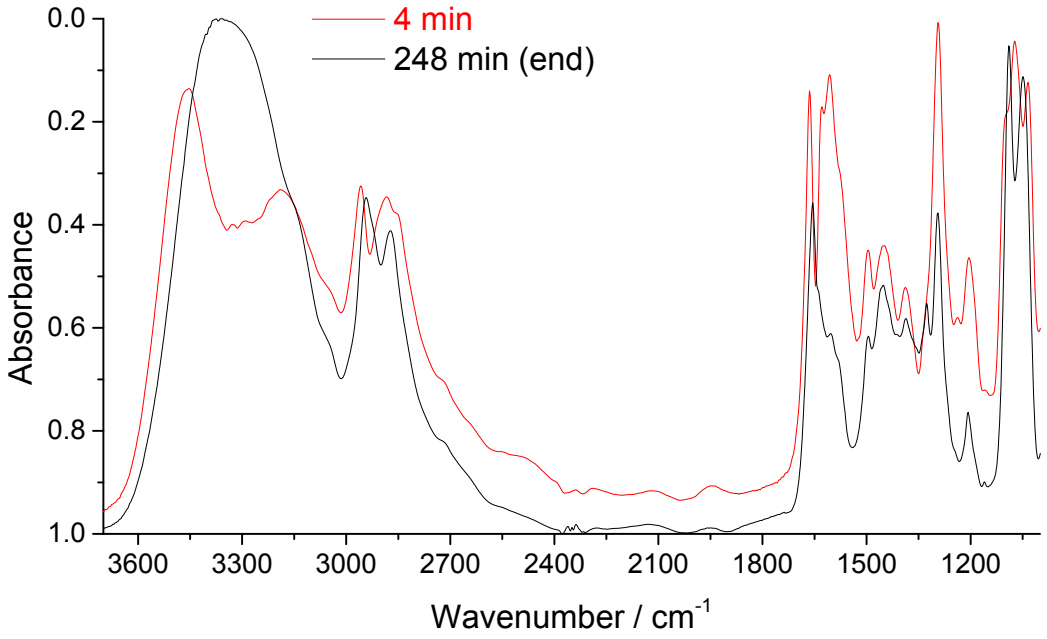

Figure S9. Normalized IR difference spectra (DS) of EG:DBU (4:1) at 4 min and at the end (248 min).

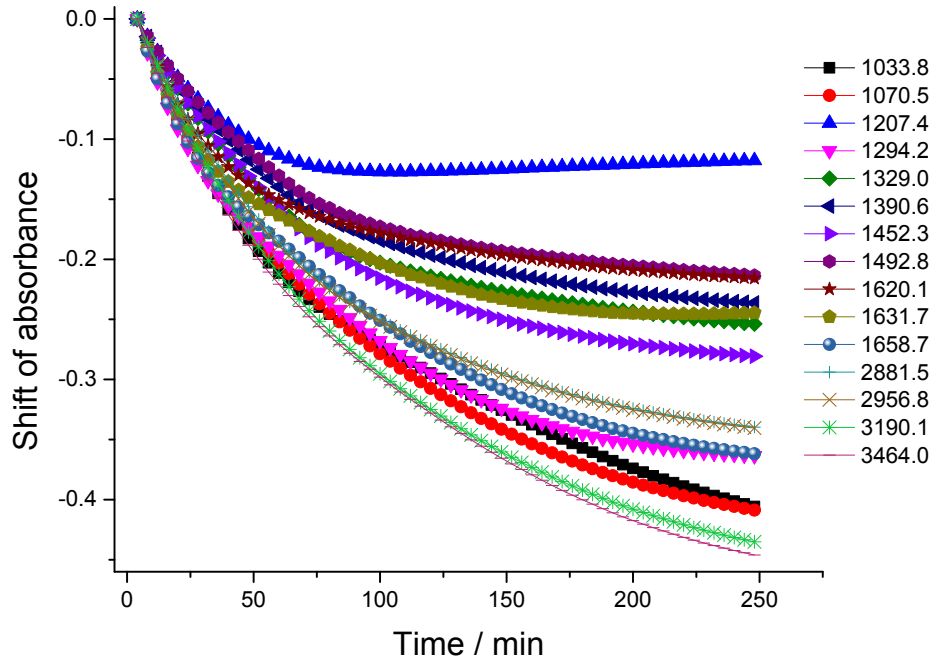

Figure S10. Shift of IR peak in difference spectra (DS) of EG:DBU (4:1) as a function of time.

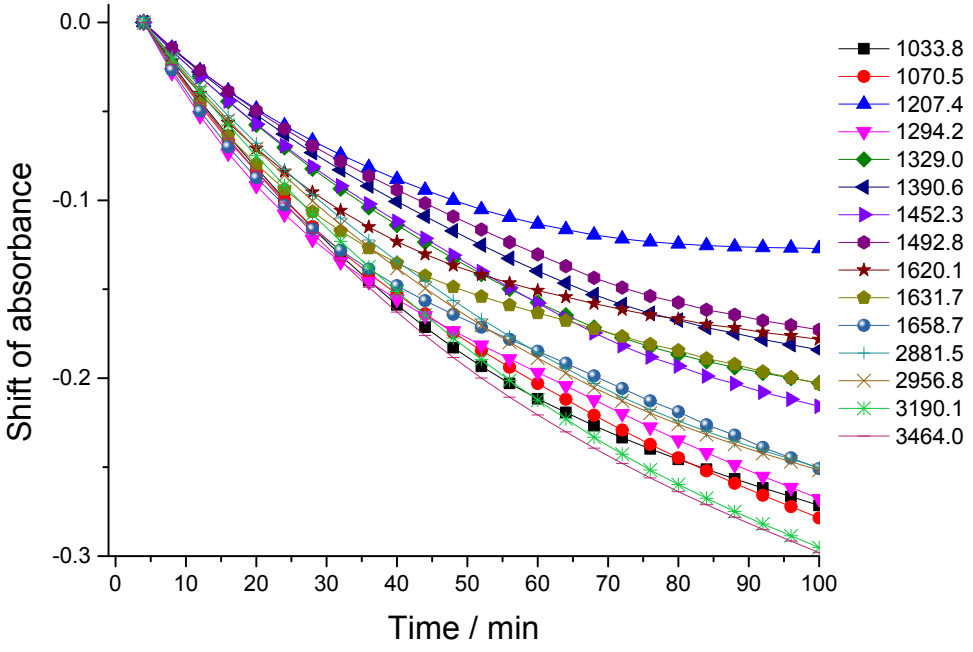

Figure S11. Expanded shift of IR peak in difference spectra (DS) of EG:DBU (4:1) as a function of time during the first 100 min.

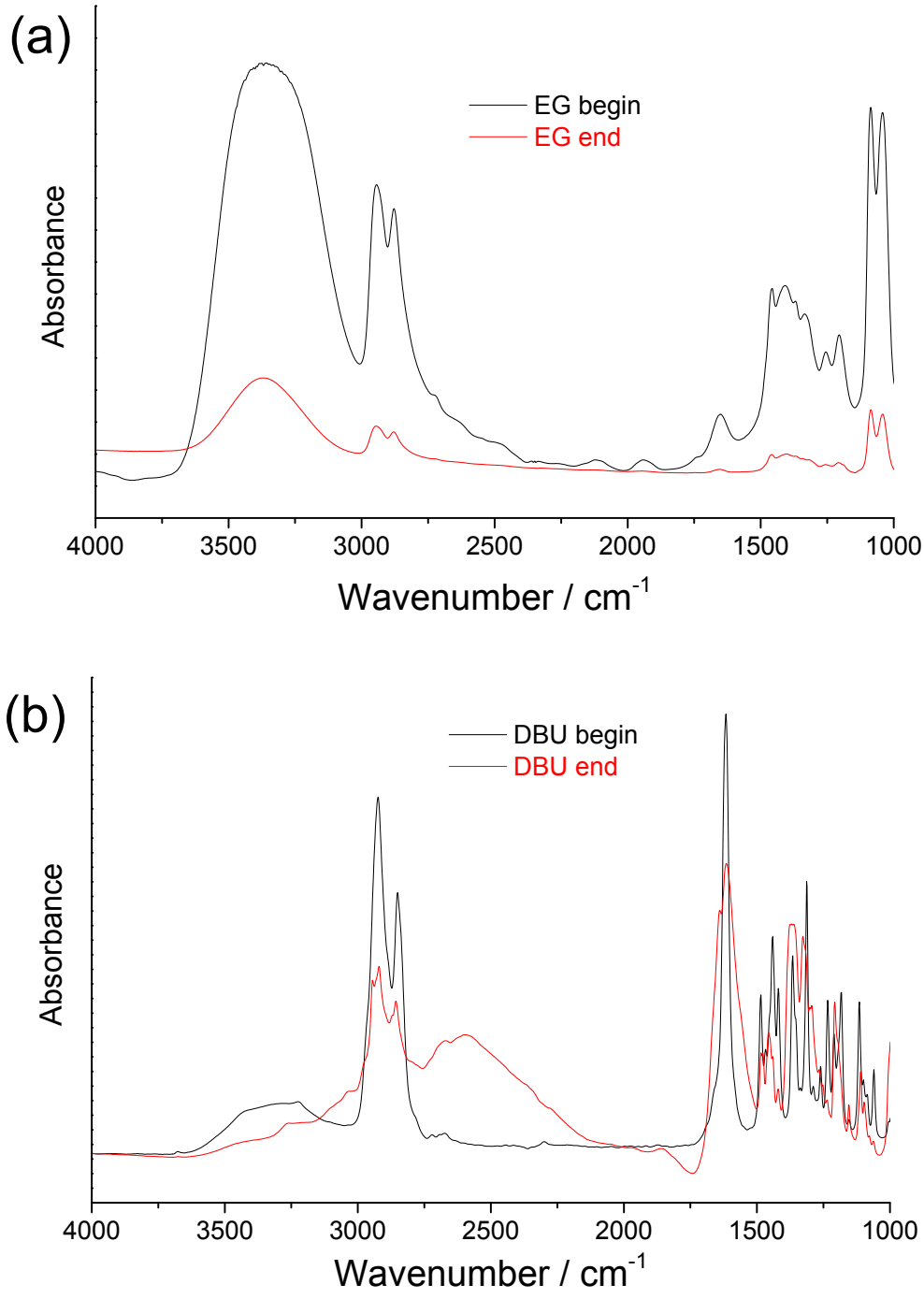

Figure S12. IR spectra of EG (a) and DBU (b) exposed to the air at the beginning at 0 min and at the end at 248 min.

Table S7. IR peaks of EG:DBU (4:1), EG:DBU (4:1)+CO_2 at the beginning and at the end.[a]

EG:DBU (4:1) at the beginning / cm^{-1}	EG:DBU (4:1)+CO_2 at the beginning / cm^{-1}	Shift after CO_2 capture / cm^{-1}	Shift after CO_2 capture	EG:DBU (4:1) at the end / cm^{-1}	EG:DBU (4:1)+CO_2 at the end / cm^{-1}	Shift after CO_2 capture / cm^{-1}	Shift after CO_2 capture
1045.4	1043.5	-1.9	→	1043.5	1045.4	1.9	←
1089.7	1087.8	-1.9	→	1089.7	1089.7	0	
1159.2	1159.2	0		1159.2	1159.2	0	
1207.4	1201.6	-5.8	→	1205.5	1201.6	-3.9	→
—	1263.3	♥	♥	1269.1	1263.3	-5.8	→
1296.1	—	♥	♥	—	—	--	
1325.0	1325.0	0		1323.1	1323.1	0	
1335.9	1354.0	18.1	←	1354.0	1354.0	0	
1367.5	1365.6	-1.9	→	—	—	--	
1386.8	1388.7	1.9	←	1386.8	1388.7	1.9	←
1448.5	1448.5	0		1446.6	1446.6	0	
1490.9	1494.8	3.9	←	—	—	--	
1649.1	1649.1	0		1647.1	1643.3	-3.8	→
2868.0	2870.0	2	←	2862.3	2860.3	-2	→
2935.6	2935.6	0		2931.7	2931.7	0	
3346.4	3356.0	9.6	←	3344.4	3356.0	11.6	←

[a] ← means blue shift of IR peak; → means red shift of IR peak; ♥ means new peak or disappeared peak with significant change of IR peak; Blank cell means no shift; — means that there is no IR peak.

Table S8. Calculated IR spectra of EG, EG/EG (1:1), DBU and EG:DBU (1:1) by DFT B3lYP/6-31++G(d, p) method.[24]

Freq. of EG	Inten. of EG	Freq. of EG/EG (1:1)	Inten. of EG/EG (1:1)	Freq. of DBU	Inten. of DBU	Freq. of EG:DBU (1:1)	Inten. of EG:DBU (1:1)	Freq. of EG:DBU (2:1)	Inten. of EG:DBU (2:1)
1063.0	237.55	1057.9	572.99	1010.5	4.45	1004.9	6.22	1005.1	6.06
1076.8	0.01	1069.0	0.01	1014.0	2.45	1013.1	8.88	1014.0	4.55
1157.2	0.03	1076.7	1.69	1069.5	14.44	1018.7	0.79	1019.2	1.35
1176.0	92.04	1081.8	0.00	1097.8	2.40	1058.8	146.78	1060.2	168.06
1224.2	1.27	1157.3	572.99	1100.7	2.69	1075.9	21.95	1063.7	216.00
1274.0	0.00	1158.0	0.01	1121.9	6.94	1096.0	65.10	1075.6	21.80
1301.4	0.00	1181.3	234.22	1133.9	21.34	1100.4	8.64	1078.3	9.39
1397.3	4.84	1199.3	0.00	1188.8	2.04	1103.5	5.06	1094.8	72.66
1476.0	0.00	1225.0	2.95	1206.4	22.99	1123.4	7.81	1100.8	6.46
1525.6	0.00	1225.2	0.98	1217.3	5.79	1132.9	21.63	1102.1	3.21
1534.1	6.83	1272.5	6.43	1229.9	17.44	1158.6	0.06	1120.8	10.41
3009.4	0.00	1296.7	0.00	1249.7	11.56	1191.1	1.95	1126.7	19.49
3014.8	113.60	1301.9	0.20	1258.2	27.81	1209.9	19.02	1157.2	1.56
3040.2	0.00	1302.1	0.00	1291.0	3.27	1216.5	48.60	1158.2	0.01
3067.1	92.35	1399.9	0.00	1296.5	4.41	1222.1	14.76	1190.5	11.14
3848.5	0.00	1401.2	10.19	1310.7	4.24	1226.2	16.54	1200.9	63.89
3849.0	71.11	1476.8	0.00	1340.9	8.51	1232.3	17.29	1215.3	28.59
		1478.3	1.37	1344.0	37.02	1255.8	7.63	1217.8	76.13
		1525.1	0.05	1363.1	5.45	1261.6	25.70	1219.8	12.86
		1525.5	0.00	1367.5	0.92	1293.6	2.61	1225.1	12.90
		1533.9	14.58	1380.0	0.09	1297.3	0.17	1226.1	1.83
		1534.1	0.02	1384.4	27.89	1301.2	4.72	1227.0	10.81
		3008.1	49.88	1396.0	35.92	1312.7	4.29	1252.0	22.04
		3008.2	0.03	1405.6	17.74	1341.4	12.64	1260.0	4.02
		3017.9	175.85	1450.4	40.36	1345.7	51.02	1292.2	13.28
		3018.3	0.01	1483.6	3.81	1351.6	8.87	1294.7	7.15
		3040.8	8.16	1489.4	0.56	1365.5	3.23	1298.1	0.07
		3040.9	0.01	1491.1	7.10	1370.8	1.31	1300.5	4.93
		3069.2	0.01	1496.4	3.46	1383.0	0.67	1302.7	0.47
		3069.5	167.88	1498.7	11.21	1387.1	25.84	1310.7	3.34
		3794.4	0.03	1505.8	12.39	1400.2	37.64	1339.0	28.76

		3803.6	235.71	1522.7	7.71	1407.0	13.12	1345.0	35.92
		3848.6	68.17	1529.5	8.58	1429.1	4.39	1353.7	8.99
		3848.7	4.59	1682.4	301.26	1458.4	47.63	1365.8	4.23
				2983.5	33.55	1487.1	3.02	1371.2	1.44
				2991.5	95.77	1489.7	5.34	1386.2	1.43
				3021.2	34.33	1493.0	1.92	1389.9	17.76
				3028.7	31.94	1497.5	2.63	1399.8	25.57
				3034.8	6.17	1502.9	12.45	1405.6	1.95
				3037.1	24.96	1507.0	9.00	1411.3	11.51
				3044.4	8.91	1509.5	8.19	1428.4	5.21
				3047.9	56.08	1522.5	7.10	1451.6	37.01
				3055.2	24.15	1523.6	3.15	1480.1	1.36
				3060.7	77.07	1530.3	9.39	1488.9	0.79
				3065.0	49.29	1533.7	11.06	1491.8	4.99
				3070.7	33.72	1674.1	410.98	1495.4	2.90
				3080.1	70.94	2976.7	55.56	1501.3	0.81
				3087.3	47.25	2994.9	23.90	1504.7	11.98
				3096.3	53.30	3001.7	87.52	1506.6	7.48
				3131.8	11.26	3005.3	31.39	1512.1	13.62
						3007.9	66.95	1523.3	0.98
						3025.5	36.83	1525.0	11.97
						3034.3	25.90	1525.5	0.08
						3039.7	20.06	1532.2	6.74
						3042.4	8.96	1533.4	12.05
						3047.4	10.24	1534.5	8.94
						3053.2	82.67	1679.3	334.59
						3056.1	25.97	2980.3	56.13
						3060.1	42.91	2933.8	37.86
						3066.8	61.44	3005.8	1.55
						3074.6	43.38	3007.9	52.25
						3075.8	30.35	3009.4	36.92
						3084.5	65.89	3010.7	98.92
						3094.0	44.13	3023.4	35.83
						3102.8	41.39	3029.1	37.28
						3134.1	3.93	3037.1	24.96
						3304.6	1704.05	3038.2	3.50
						3847.3	29.27	3039.0	19.26
								3046.9	10.19
								3054.3	81.63
								3055.3	10.46
								3062.1	1.10

								3064.5	84.52
								3064.8	55.06
								3075.4	42.61
								3078.1	39.41
								3084.4	37.88
								3085.8	57.06
								3097.8	36.36
								3119.1	23.72
								3136.9	2.25
								3361.2	1622.50
								3720.8	416.25
								3847.7	40.08
								3847.8	27.85

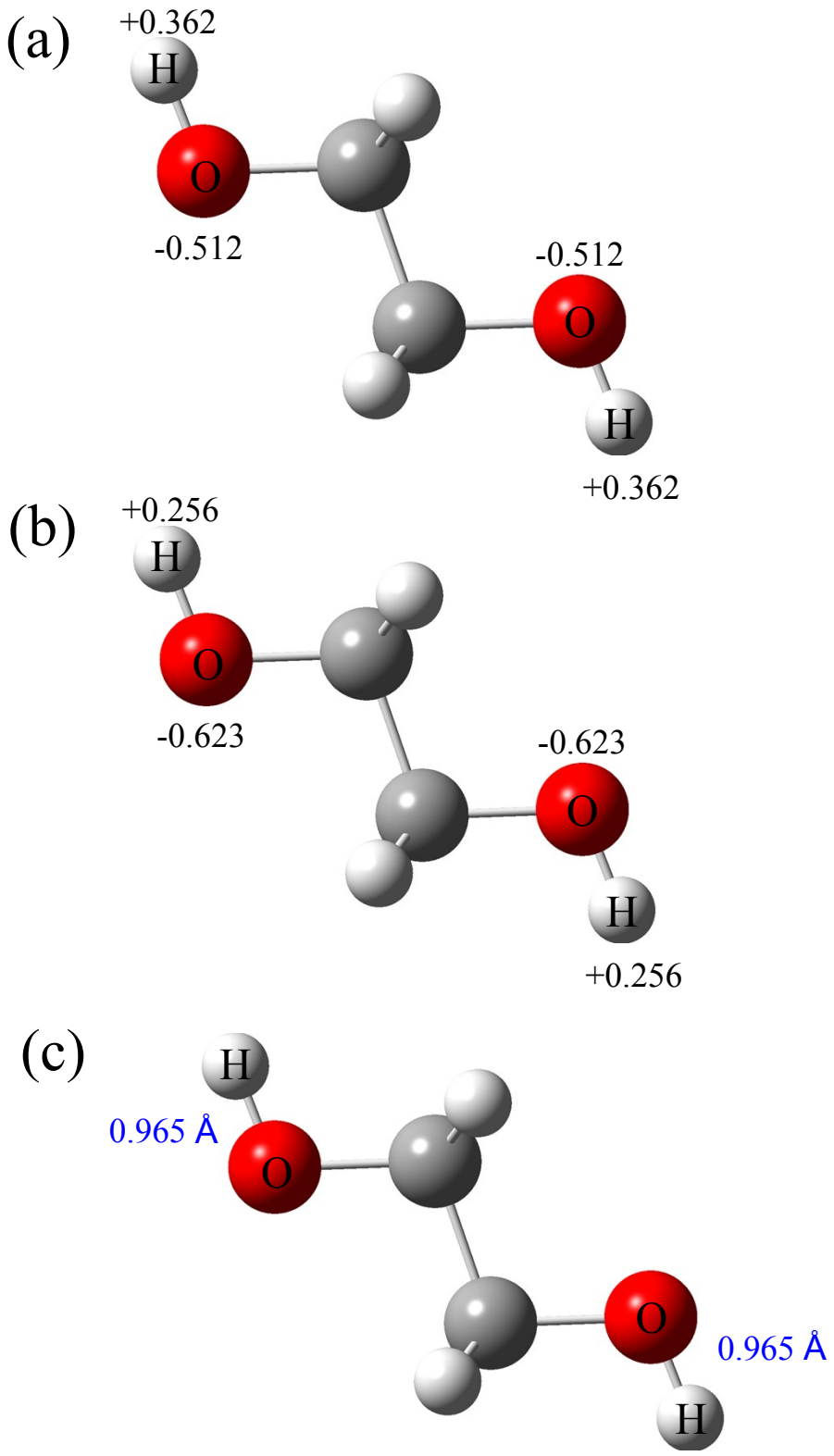

Figure S1. Calculated Mulliken charge (a), APT charge (b) and O-H bond length (c) of EG by DFT B3lYP/6-31++G(d, p) method. Black and blue numbers are charge and bond length, respectively.

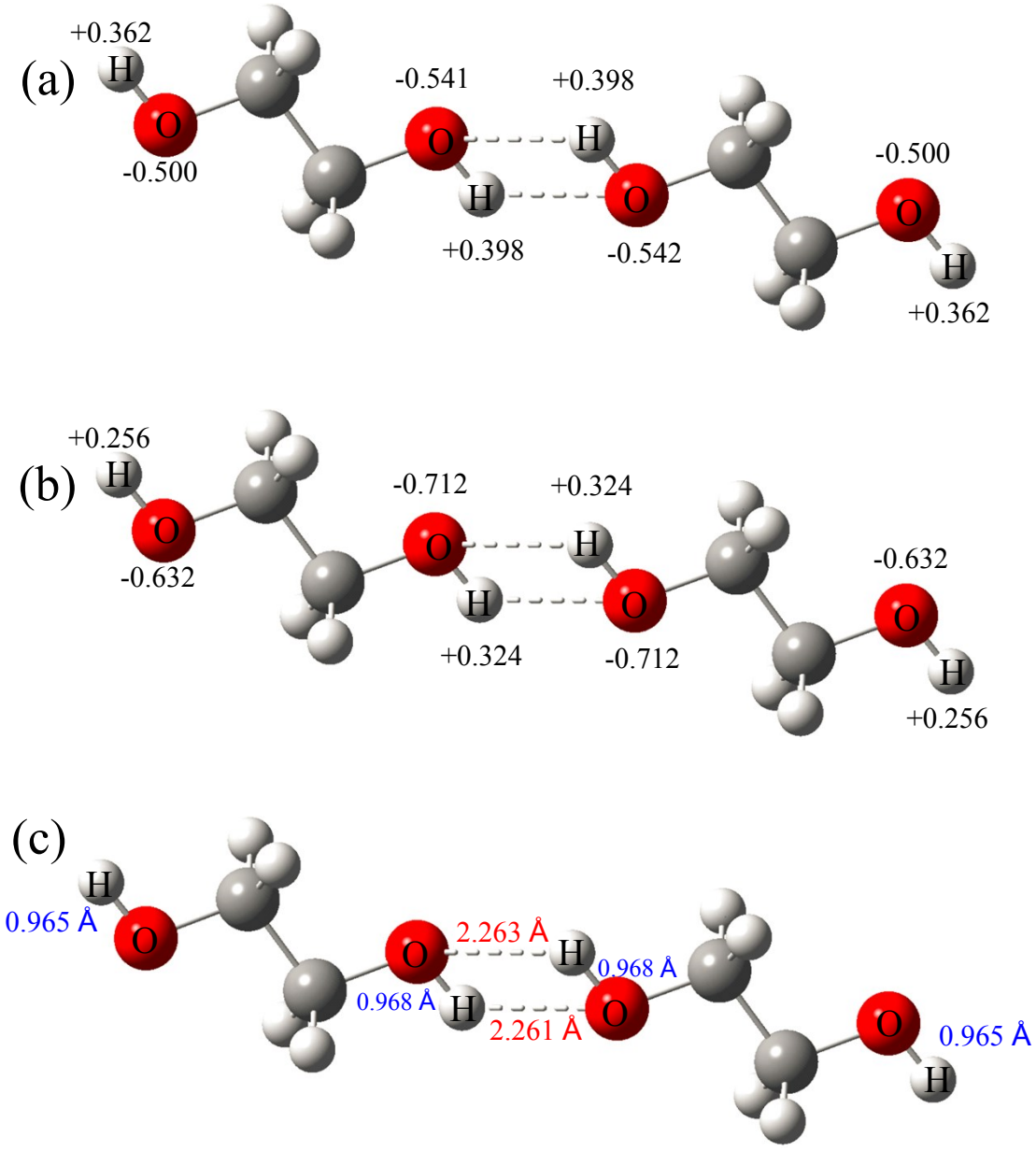

Figure S2. Calculated Mulliken charge (a) APT charge (b) and O-H bond length (c) of EG/EG (1:1) by DFT B3lYP/6-31++G(d, p) method. Black, blue and red numbers are charge, intramolecular bond length and intermolecular hydrogen-bond length, respectively. The intermolecular hydrogen-bond is also marked with dashed line.

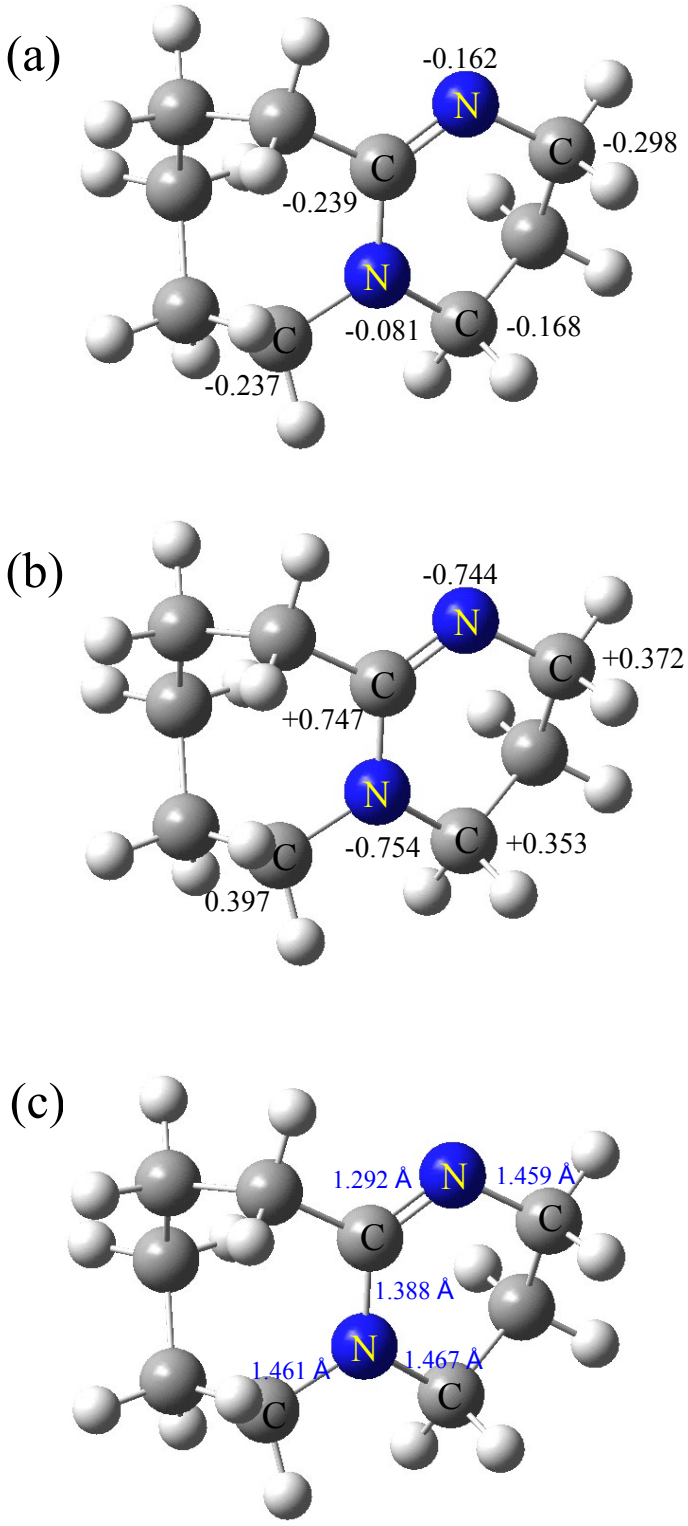

Figure S3. Calculated Mulliken charge (a), APT charge (b) and C-N bond length (c) of DBU by DFT B3lYP/6-31++G(d, p) method. Black and blue numbers are charge and bond length, respectively.

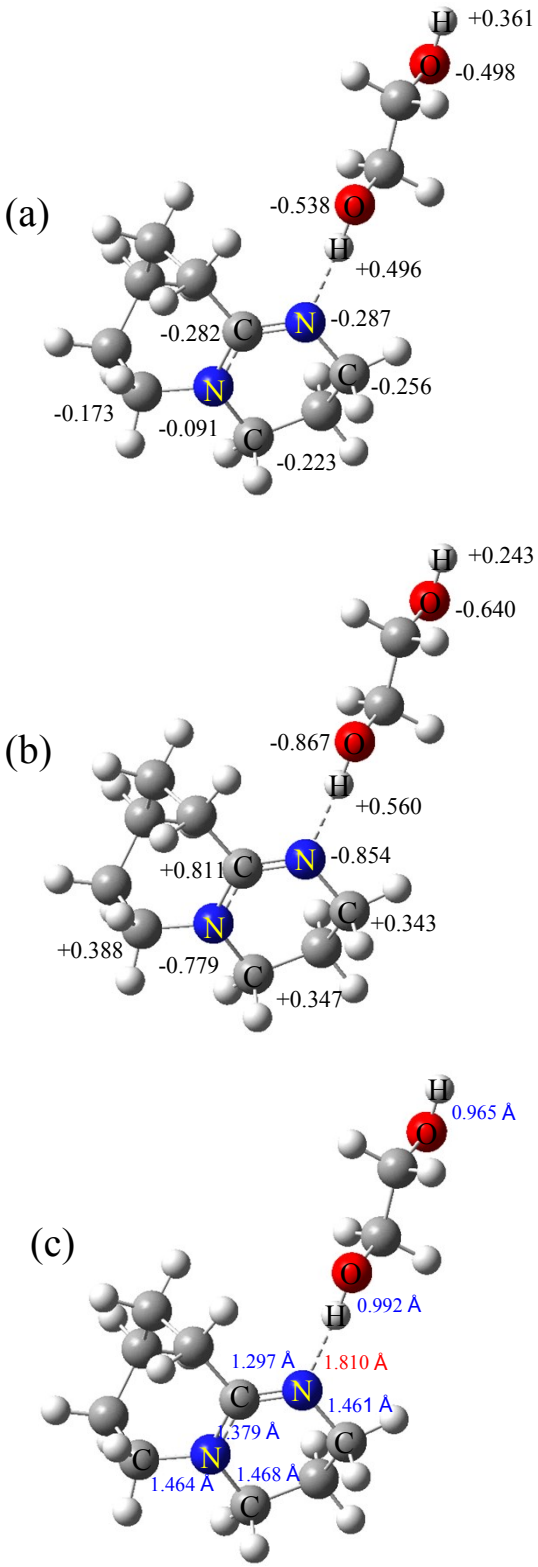

Figure S4. Calculated Mulliken charge (a), APT charge (b) and bond length (c) of EG:DBU (1:1) by DFT B3lYP/6-31++G(d, p) method. Black, blue and red numbers are charge, intramolecular bond length and intermolecular hydrogen-bond length, respectively. The intermolecular hydrogen-bond is also marked with dashed line.

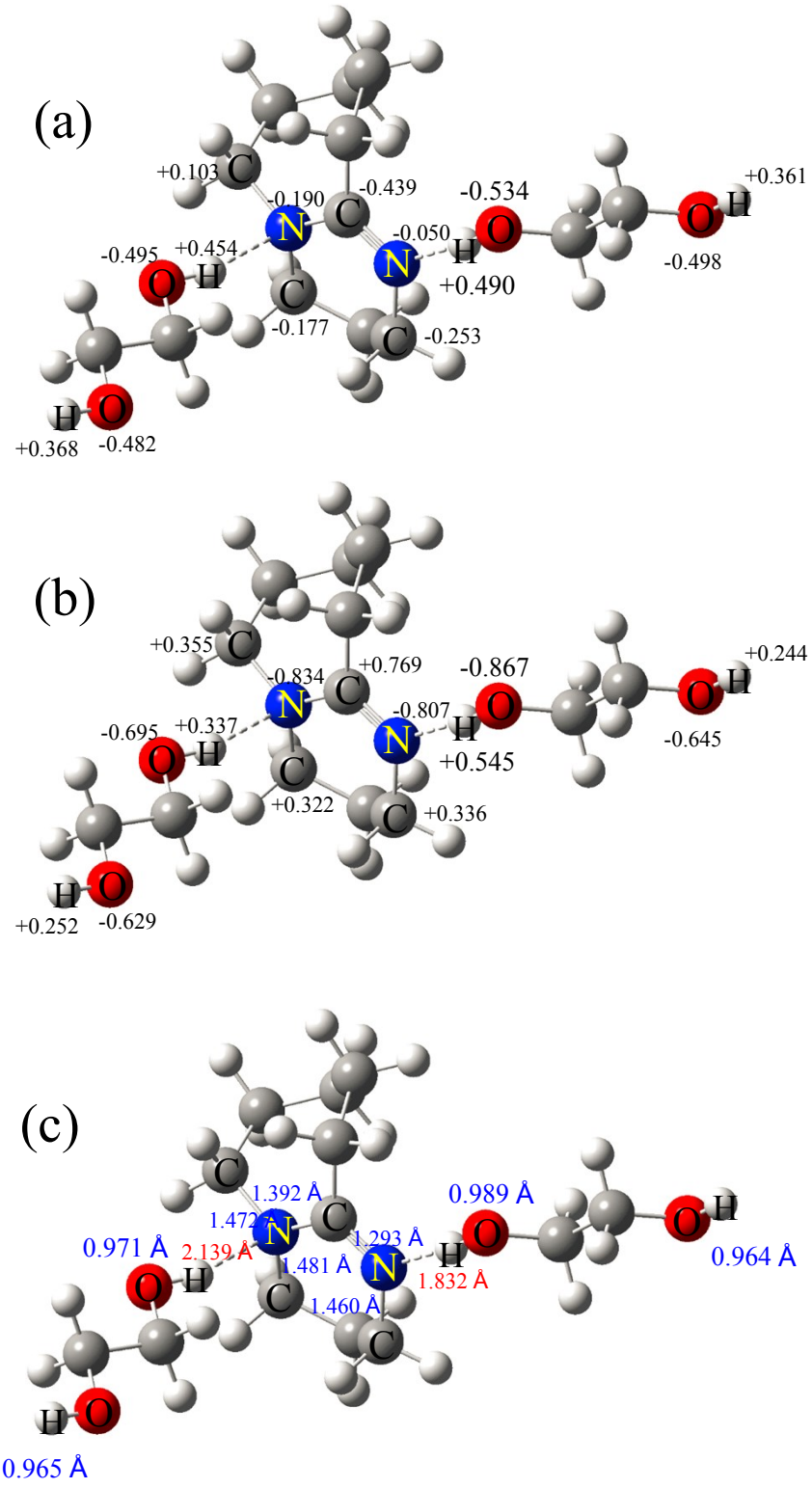

Figure S5. Calculated Mulliken charge (a), APT charge (b) and bond length (c) of EG:DBU (2:1) by DFT B3lYP/6-31++G(d, p) method. Black, blue and red numbers are charge, intramolecular bond length and intermolecular hydrogen-bond length, respectively. The intermolecular hydrogen-bond is also marked with dashed line.

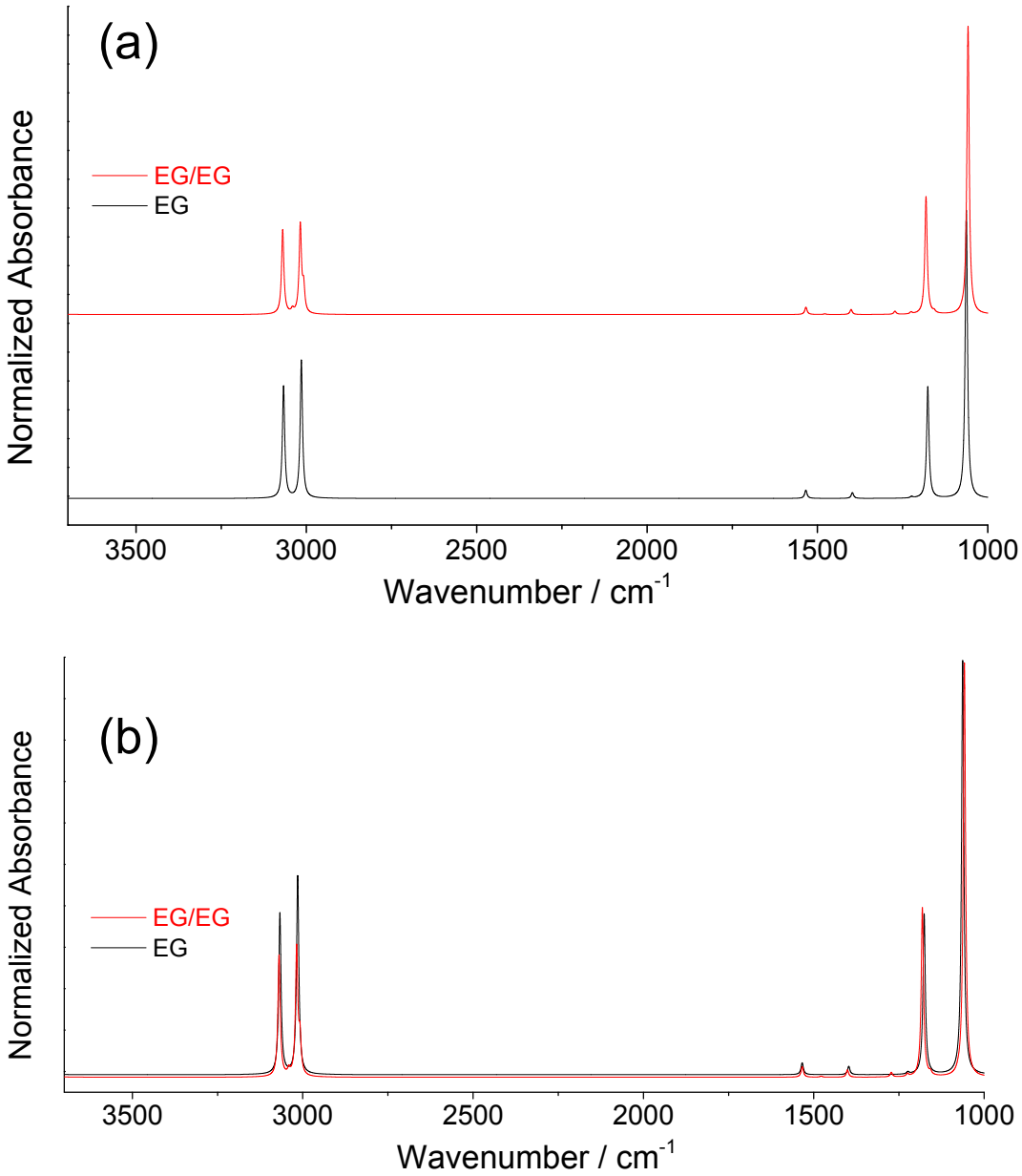

Figure S6. Comparison of calculated infrared spectra of EG and EG/EG (1:1) by DFT B3lYP/6-31++G(d, p) method. Separate comparison (a) and converged comparison (b).

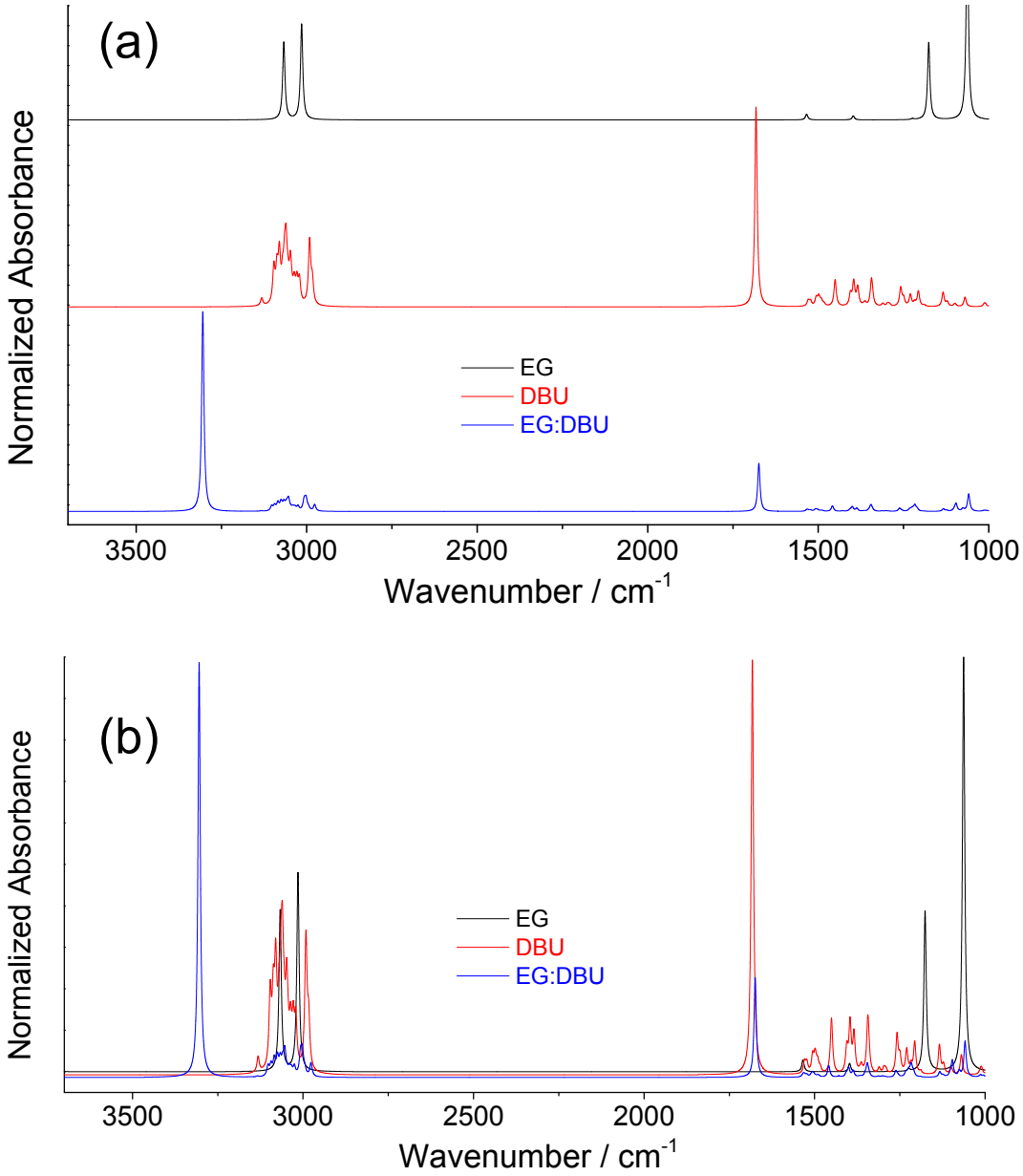

Figure S7. Comparison of calculated infrared spectra of EG, DBU and EG:DBU (1:1) by DFT B3lYP/6-31++G(d, p) method. Separate comparison (a) and converged comparison (b).

Table S9. Cartesian coordinates of all the optimized species by the Gaussian calculation (i.e., output file) for EG by DFT B3lYP/6-31++G(d, p) method.

C	0.87645000	0.26801800	0.00351400
C	1.37248400	-1.16935300	-0.00023800
H	1.26045400	0.78750600	-0.88528300
H	1.25809100	0.78200500	0.89649400
H	0.98847400	-1.68895000	0.88851000
H	0.99090200	-1.68328500	-0.89326000
O	2.79961900	-1.11726600	0.00190700
H	3.15015400	-2.01596200	-0.00046600
O	-0.55074800	0.21609900	0.00174300
H	-0.90103100	1.11489400	-0.00100000

1 2 1.0 3 1.0 4 1.0 9 1.0

2 5 1.0 6 1.0 7 1.0

3

4

5

6

7 8 1.0

8

9 10 1.0

10

Table S10. Cartesian coordinates of all the optimized species by the Gaussian calculation (i.e., output file) for DBU by DFT B3lYP/6-31++G(d, p) method.

C	-4.76195000	-0.60100900	-0.17140000
C	-2.64371400	0.27894600	0.34499800
C	-3.31941500	1.06879400	1.47092400
C	-4.66779500	1.59393900	0.98099500
H	-1.70286500	-0.15972300	0.69582000
H	-3.47143400	0.40575100	2.33157500
H	-2.69529700	1.90507600	1.80578100
H	-5.27159000	1.94180200	1.82874700
H	-4.52071000	2.45767100	0.31419600
H	-2.37927100	0.96178700	-0.47864300
C	-6.58882700	-2.38110800	0.32569700
C	-5.65401900	-1.70009800	-0.71936000
C	-6.92087600	-1.54470100	1.57400000
C	-7.59430600	-0.18823200	1.30888400
C	-6.86588300	0.65166900	0.23384200
H	-7.51766800	-2.68620700	-0.17359600
H	-4.98080200	-2.43942800	-1.15606600
H	-5.99310500	-1.37260900	2.13290300
H	-7.63956100	0.36986100	2.25307300
H	-6.10823500	-3.30461700	0.66803100
H	-6.25136500	-1.29469700	-1.54477000
H	-7.56474700	-2.13703600	2.23596600
H	-8.63393100	-0.33139200	0.98395200
H	-7.12176800	1.71077900	0.34433200
H	-7.21842800	0.36237300	-0.76083700
N	-3.48525000	-0.79609100	-0.16954800

N -5.40935500 0.54294800 0.27588600

1 12 1.0 26 2.0 27 1.0

2 3 1.0 5 1.0 10 1.0 26 1.0

3 4 1.0 6 1.0 7 1.0

4 8 1.0 9 1.0 27 1.0

5

6

7

8

9

10

11 12 1.0 13 1.0 16 1.0 20 1.0

12 17 1.0 21 1.0

13 14 1.0 18 1.0 22 1.0

14 15 1.0 19 1.0 23 1.0

15 24 1.0 25 1.0 27 1.0

16

17

18

19

20

21

22

23

24

25

26

27

Table S11. Cartesian coordinates of all the optimized species by the Gaussian calculation (i.e., output file) for EG/EG (1:1) by DFT B3lYP/6-31++G(d, p) method.

C	-3.23185100	-0.31344200	0.07772400
C	-2.51730800	-1.65553600	0.07320600
H	-3.02738300	0.21314300	-0.86431500
H	-2.85039200	0.29780100	0.90659000
H	-2.72230600	-2.17960600	1.01698700
H	-2.90004700	-2.26935800	-0.75435900
O	-1.12368500	-1.38478800	-0.08126200
H	-0.63752300	-2.21792500	-0.08655600
O	-4.62693200	-0.57780000	0.23214200
H	-5.11763800	0.25600100	0.26073800
C	-9.15599500	1.31873500	-0.75002300
C	-8.43752000	-0.02126800	-0.75463400
H	-8.96178300	1.83843900	-1.69848600
H	-8.76696400	1.93800100	0.07052700
H	-8.63090100	-0.54350200	0.19216000
H	-8.82548900	-0.63798500	-1.57639500
O	-7.04487400	0.24642600	-0.92447000
H	-6.55218900	-0.58619400	-0.95387200
O	-10.54722500	1.04479200	-0.58044100
H	-11.03578800	1.87652200	-0.57506700

1 2 1.0 3 1.0 4 1.0 9 1.0

2 5 1.0 6 1.0 7 1.0

3

4

5

6

7 8 1.0

8

9 10 1.0

10

11 12 1.0 13 1.0 14 1.0 19 1.0

12 15 1.0 16 1.0 17 1.0

13

14

15

16

17 18 1.0

18

19 20 1.0

20

Table S12. Cartesian coordinates of all the optimized species by the Gaussian calculation (i.e., output file) for DBU/DBU (1:1) by DFT B3lYP/6-31++G(d, p) method.

C	-2.50618900	0.34087800	0.19132900
C	-0.48234000	-0.08736600	1.31833400
C	-1.30533500	-0.23329000	2.60200400
C	-2.40465200	0.82683200	2.61980300
H	0.26690900	-0.88433400	1.25268700
H	-1.75551600	-1.23322400	2.62923600
H	-0.67621900	-0.13114600	3.49320000
H	-3.14406500	0.59650300	3.39664100
H	-1.97916300	1.81310600	2.86049400
H	0.07747700	0.86123200	1.34304400
C	-4.61900900	-0.60016100	-0.99953100
C	-3.36602700	0.32513900	-1.05947000
C	-5.13638700	-0.93709500	0.40980900
C	-5.53681200	0.26817600	1.27648900
C	-4.46466500	1.38210200	1.30219700
H	-5.42408300	-0.14647400	-1.59164600
H	-2.70886500	0.00868200	-1.87078200
H	-4.36212500	-1.50781400	0.93651600
H	-5.73315100	-0.08469800	2.29708900
H	-4.37310800	-1.54682800	-1.49379100
H	-3.67204900	1.35235700	-1.29080000
H	-5.99719000	-1.61082600	0.31942700
H	-6.47608700	0.70726800	0.91404500
H	-4.59959600	2.01609200	2.18449100
H	-4.59490600	2.04163100	0.43874500
N	-1.30462400	-0.13171200	0.11192900
N	-3.08972300	0.88446500	1.32383500

C	2.74100800	-1.89366400	-3.25656300
C	3.51901200	0.32519900	-3.24163700
C	2.34510000	0.65849700	-2.31492800
C	1.09946600	-0.09417200	-2.77876400
H	4.43821300	0.80722000	-2.88875500
H	2.59926500	0.35554100	-1.29140000
H	2.14131300	1.73543900	-2.29697100
H	0.32489600	-0.07113200	-2.00352200
H	0.68331300	0.38573300	-3.67899600
H	3.32230700	0.73324900	-4.24674800
C	2.68594300	-4.20937000	-2.07904200
C	2.97645600	-3.38906900	-3.37238300
C	1.70800900	-3.56188500	-1.08202400
C	0.30917600	-3.23831000	-1.63160900
C	0.34740800	-2.47642600	-2.97611700
H	2.31976100	-5.20471100	-2.36349400
H	4.02251800	-3.50475500	-3.66069300
H	2.16024300	-2.63514700	-0.70828700
H	-0.23453300	-2.63823200	-0.89246700
H	3.63406200	-4.37132700	-1.55317600
H	2.37668300	-3.77999600	-4.20312200
H	1.60482300	-4.22004500	-0.20986700
H	-0.26717700	-4.16260700	-1.77929900
H	-0.59607900	-1.94187700	-3.12560800
H	0.42810200	-3.18617900	-3.80591700
N	3.76601100	-1.10955500	-3.34117900
N	1.42617900	-1.49568800	-3.07878700

1 12 1.0 26 2.0 27 1.0

2 3 1.0 5 1.0 10 1.0 26 1.0

3 4 1.0 6 1.0 7 1.0

4 8 1.0 9 1.0 27 1.0

5

6

7

8

9

10

11 12 1.0 13 1.0 16 1.0 20 1.0

12 17 1.0 21 1.0

13 14 1.0 18 1.0 22 1.0

14 15 1.0 19 1.0 23 1.0

15 24 1.0 25 1.0 27 1.0

16

17

18

19

20

21

22

23

24

25

26

27

28 39 1.0 53 2.0 54 1.0

29 30 1.0 32 1.0 37 1.0 53 1.0

30 31 1.0 33 1.0 34 1.0

31 35 1.0 36 1.0 54 1.0

32

33

34

35

36

37

38 39 1.0 40 1.0 43 1.0 47 1.0

39 44 1.0 48 1.0

40 41 1.0 45 1.0 49 1.0

41 42 1.0 46 1.0 50 1.0

42 51 1.0 52 1.0 54 1.0

43

44

45

46

47

48

49

50

51

52

53

54

Table S13. Cartesian coordinates of all the optimized species by the Gaussian calculation (i.e., output file) for EG:DBU (1:1) by DFT B3lYP/6-31++G(d, p) method.

C	-3.85216900	0.71090100	-0.14791900
C	-1.81449500	1.87381100	0.16998500
C	-2.42846500	2.45647200	1.44524000
C	-3.89534300	2.79618400	1.18943100
H	-0.78304300	1.55271200	0.35000000
H	-2.35461600	1.71654700	2.25129800
H	-1.89160000	3.35391600	1.77116300
H	-4.41355300	2.98756300	2.13677200
H	-3.97652900	3.71209300	0.58499100
H	-1.76791500	2.64864700	-0.61089500
C	-5.32101500	-1.36755800	0.37490500
C	-4.64520200	-0.46000100	-0.69781500
C	-5.57031300	-0.71646100	1.74667400
C	-6.45158300	0.54357500	1.73582800
C	-6.02355100	1.57453400	0.66734800
H	-6.26594900	-1.74981600	-0.03148900
H	-3.95444400	-1.05150400	-1.30059900
H	-4.60106800	-0.46431300	2.19385600
H	-6.41968500	1.00250000	2.73226400
H	-4.68210000	-2.24266300	0.53627100
H	-5.40232500	-0.07006300	-1.38815800
H	-6.02264900	-1.45987500	2.41420000
H	-7.50096200	0.27807600	1.55016400
H	-6.40561700	2.56812600	0.92226100
H	-6.47308500	1.31852600	-0.29641400
N	-2.56854200	0.72783100	-0.33251900

N	-4.57368200	1.69001000	0.50264400
C	-0.52587500	-2.11022600	-0.58306300
C	-0.01467300	-3.40230100	-1.20192600
H	0.33613800	-1.52126300	-0.23079400
H	-1.14151500	-2.35533800	0.29678500
H	-0.86865900	-4.00268500	-1.54597000
H	0.61206700	-3.16332800	-2.07227500
O	0.73537500	-4.09862500	-0.19946800
H	1.10701300	-4.89990000	-0.58674700
O	-1.26776600	-1.42009300	-1.57032600
H	-1.70298800	-0.63181700	-1.15510800

1 12 1.0 26 2.0 27 1.5

2 3 1.0 5 1.0 10 1.0 26 1.0

3 4 1.0 6 1.0 7 1.0

4 8 1.0 9 1.0 27 1.0

5

6

7

8

9

10

11 12 1.0 13 1.0 16 1.0 20 1.0

12 17 1.0 21 1.0

13 14 1.0 18 1.0 22 1.0

14 15 1.0 19 1.0 23 1.0

15 24 1.0 25 1.0 27 1.0

16

17

18

19

20

21

22

23

24

25

26

27

28 29 1.0 30 1.0 31 1.0 36 1.0

29 32 1.0 33 1.0 34 1.0

30

31

32

33

34 35 1.0

35

36 37 1.0

37

Table S14. Cartesian coordinates of all the optimized species by the Gaussian calculation (i.e., output file) for EG:DBU (2:1) by DFT B3lYP/6-31++G(d, p) method.

C	-4.16278100	0.78868400	1.11316300
C	-2.67248600	2.22241300	-0.01820600
C	-2.18820000	2.69504500	1.35463800
C	-3.38510000	2.84098800	2.29265200
H	-1.82986400	2.07906300	-0.70163900
H	-1.48443700	1.95471300	1.75291300
H	-1.65663800	3.64999000	1.28568900
H	-3.04977500	2.84584100	3.33670100
H	-3.90186700	3.79355600	2.11592000
H	-3.31903400	2.98945500	-0.47365000
C	-4.51146400	-1.42509500	2.41138800
C	-4.95001500	-0.50088100	1.23357300
C	-3.72727900	-0.73842000	3.54343400
C	-4.46836400	0.39828500	4.26781300
C	-5.14968900	1.39476300	3.30772500
H	-5.39908200	-1.92181800	2.82259200
H	-4.83504100	-1.02805000	0.28538700
H	-2.78975400	-0.34621800	3.12926600
H	-3.75896600	0.92443300	4.91908500
H	-3.87716600	-2.22008900	2.00478300
H	-6.01360000	-0.25290800	1.32385900
H	-3.43161900	-1.49499100	4.27999300
H	-5.24509200	-0.01053700	4.92737600
H	-5.37356900	2.33403100	3.82274700
H	-6.11359300	0.99989800	2.97974000
N	-3.40295100	0.96220300	0.08087200
N	-4.35349100	1.73474500	2.11672200

C	-2.10429000	-1.46612900	-2.20250600
C	-2.21009100	-2.59128400	-3.22060200
H	-1.43598000	-0.68742600	-2.60260800
H	-1.64464000	-1.85954600	-1.28221100
H	-2.87221800	-3.37522400	-2.82681000
H	-2.65143600	-2.20000100	-4.14765100
O	-0.88948300	-3.09634000	-3.44822500
H	-0.93006600	-3.78807000	-4.11906100
O	-3.41015600	-0.97074200	-1.97040200
H	-3.37422400	-0.26557400	-1.27847900
C	-8.28118700	4.41869800	-0.36659300
C	-6.93557700	3.72053600	-0.24689200
H	-8.33320600	5.23285700	0.37001000
H	-9.08444400	3.70171400	-0.14718100
H	-6.89295900	2.88351300	-0.95668500
H	-6.13871800	4.43213800	-0.50682800
O	-6.81326200	3.26968900	1.10124900
H	-5.98694400	2.77061200	1.20426200
O	-8.37815300	4.91809400	-1.70152600
H	-9.24093200	5.33205900	-1.82245600

1 12 1.0 26 2.0 27 1.0

2 3 1.0 5 1.0 10 1.0 26 1.0

3 4 1.0 6 1.0 7 1.0

4 8 1.0 9 1.0 27 1.0

5

6

7

8

9

10

11 12 1.0 13 1.0 16 1.0 20 1.0

12 17 1.0 21 1.0

13 14 1.0 18 1.0 22 1.0

14 15 1.0 19 1.0 23 1.0

15 24 1.0 25 1.0 27 1.0

16

17

18

19

20

21

22

23

24

25

26

27

28 29 1.0 30 1.0 31 1.0 36 1.0

29 32 1.0 33 1.0 34 1.0

30

31

32

33

34 35 1.0

35

36 37 1.0

37

38 39 1.0 40 1.0 41 1.0 46 1.0

39 42 1.0 43 1.0 44 1.0

40

41

42

43

44 45 1.0

45

46 47 1.0

47

Table S15. Comparison of interaction enthalpy energy for EG/EG (1:1), DBU:DBU (1:1), EG:DBU (1:1) and EG:DBU (2:1) via Gaussian calculation by B3LYP/6-31++g(d, p) method.

Interaction enthalpy energy	Unit	EG/EG (1:1)	DBU/DBU (1:1)	EG:DBU (1:1)	EG:DBU (2:1)
ΔE	kJ mol^{-1}	-13.3	-3.1	-34.3	-39.2

References:

(1) Dionisio, M. S., Ramos, J. J. M. & Goncalves, R. M., The enthalpy and entropy of cavity formation in liquids and corresponding states principle. *Can. J. Chem.* **1990**, 68, 1937-1949.

(2) Emel'yanenko, V. N., Boeck, G., Verevkin, S. P. & Ludwig, R., Volatile Times for the Very First Ionic Liquid: Understanding the Vapor Pressures and Enthalpies of Vaporization of Ethylammonium Nitrate. *Chem. Eur. J.* **2014**, 20, 11640-11645.

(3) Garist, I. V., Verevkin, S. P., Bara, J. E., Hindman, M. S. & Danielsen, S. P. O., Building Blocks for Ionic Liquids: Vapor Pressures and Vaporization Enthalpies of 1-(n-Alkyl)-benzimidazoles. *J. Chem. Eng. Data* **2012**, 57, 1803-1809.

(4) Douglas, T. B., Vapor Pressure of Methyl Sulfoxide from 20 to 50°. Calculation of the Heat of Vaporization. *J. Am. Chem. Soc.* **1948**, 70, 2001-2002.

(5) M., S. R. & Stanislaw, M., Handbook of the thermodynamics of organic compounds. Richard M. Stephenson, and Stanislaw Malanowski, Elsevier, New York, 1987, 552 pp., $69.00. *AIChE J.* 35, 877-877.

(6) Ren, N.-n., Gong, Y.-h., Lu, Y.-z., Meng, H. & Li, C.-x., Surface Tension Measurements for Seven Imidazolium-Based Dialkylphosphate Ionic Liquids and Their Binary Mixtures with Water (Methanol or Ethanol) at 298.15 K and 1 atm. *J. Chem. Eng. Data* **2014**, 59, 189-196.

(7) https://macro.lsu.edu/howto/solvents/Vapor%20Pressure.htm (Accessed: June 3, 2019).

(8) Guan, W., Tong, J., Chen, S.-P., Liu, Q.-S. & Gao, S.-L., Density and Surface Tension of Amino Acid Ionic Liquid 1-Alkyl-3-methylimidazolium Glutamate. *J. Chem. Eng. Data* **2010**, 55, 4075-4079.

(9) Zaitsau, D. H., Kabo, G. J., Strechan, A. A., Paulechka, Y. U., Tschersich, A., Verevkin, S. P. & Heintz, A., Experimental vapor pressures of 1-alkyl-3-methylimidazolium bis(trifluoromethylsulfonyl) imides and a correlation scheme for estimation of vaporization enthalpies of ionic liquids. *J. Phys. Chem. A* **2006**, 110, 7303-7306.

(10) Kurnia, K. A., Mutalib, M. I. A., Man, Z. & Bustam, M. A., Density and Surface Tension of Ionic Liquids $[H_2N\text{-}C_2mim][PF_6]$ and $[H_2N\text{-}C_3mim][PF_6]$. *J. Chem. Eng. Data* **2012**, 57, 2923-2927.

(11) Paulechka, Y. U., Zaitsau, D. H., Kabo, G. J. & Strechan, A. A., Vapor pressure and thermal stability of ionic liquid 1-butyl-3-methylimidazolium Bis(trifluoromethylsulfonyl)amide. *Thermochim. Acta.* **2005**, 439, 158-160.

(12) Liu, Q.-S., Tong, J., Tan, Z.-C., Welz-Biermann, U. & Yang, J.-Z., Density and Surface Tension of

Ionic Liquid [C_2mim][$PF_3(CF_2CF_3)_3$] and Prediction of Properties [$C_n$mim][$PF_3(CF_2CF_3)_3$] (n=1, 3, 4, 5, 6). *J. Chem. Eng. Data* **2010**, 55, 2586-2589.

(13) Tong, J., Qu, Y., Jing, L., Liu, L. & Liu, C., Measurement of Vapor Pressure and Vaporization Enthalpy for Ionic Liquids 1-Hexyl-3-methylimidazolium Threonine Salt C(6)mim Thr by Isothermogravimetric Analysis. *Acta Phys-Chim. Sin.* **2018**, 34, 194-200.

(14) Zhang, Z., Wei, J., Ma, X., Xu, W., Tong, J., Guan, W. & Yang, J., The measurement of vapor pressure, enthalpy of vaporization and the prediction of the polarity for 1-propyl-3-methylimidazolium acetate C_3mim OAc ionic liquid. *Scientia Sinica Chimica* **2014**, 44, 1005-1013.

(15) Yu, G., Chen, X., Asumana, C., Zhang, S., Liu, X. & Zhou, G., Vaporization Enthalpy and Cluster Species in Gas Phase of 1,1,3,3-Tetramethylguanidinium-Based Ionic Liquids from Computer Simulations. *AIChE J.* **2011**, 57, 507-516.

(16) Ludwig, R. & Kragl, U., Do we understand the volatility of ionic liquids? *Angew. Chem. Int. Ed.* **2007**, 46, 6582-6584.

(17) Zaitsau, D. H., Emel'yanenko, V. N., Stange, P., Schick, C., Verevkin, S. P. & Ludwig, R., Dispersion and Hydrogen Bonding Rule: Why the Vaporization Enthalpies of Aprotic Ionic Liquids Are Significantly Larger than those of Protic Ionic liquids. *Angew. Chem. Int. Ed.* **2016**, 55, 11682-11686.

(18) Heym, F., Korth, W., Thiessen, J., Kern, C. & Jess, A., Evaporation and Decomposition Behavior of Pure and Supported Ionic Liquids under Thermal Stress. *Chem. Ing. Tech.* **2015**, 87, 791-802.

(19) Zaitsau, D. H., Fumino, K., Emel'yanenko, V. N., Yermalayeu, A. V., Ludwig, R. & Verevkin, S. P., Structure-Property Relationships in Ionic Liquids: A Study of the Anion Dependence in Vaporization Enthalpies of Imidazolium-Based Ionic Liquids. *ChemPhysChem* **2012**, 13, 1868-1876.

(20) Ribeiro, F. M. S., Lima, C. F. R. A. C., Vaz, I. C. M., Rodrigues, A. S. M. C., Sapei, E., Melo, A., Silva, A. M. S. & Santos, L. M. N. B. F., Vaporization of protic ionic liquids derived from organic superbases and short carboxylic acids. *Phys. Chem. Chem. Phys.* **2017**, 19, 16693-16701.

(21) Zaitsau, D. H., Yermalayeu, A. V., Emel'yanenko, V. N., Verevkin, S. P., Welz-Biermann, U. & Schubert, T., Structure-property relationships in ILs: A study of the alkyl chain length dependence in vaporisation enthalpies of pyridinium based ionic liquids. *Sci. China Chem.* **2012**, 55, 1525-1531.

(22) Yermalayeu, A. V., Zaitsau, D. H., Loor, M., Schaumann, J., Emel'yanenko, V. N., Schulz, S. & Verevkin, S. P., Imidazolium Based Ionic Liquids: Impact of the Cation Symmetry and Alkyl Chain Length on the Enthalpy of Vaporization. *Z. Anorg. Allg. Chem.* **2017**, 643, 81-86.

(23) Shahbaz, K., Mjalli, F. S., Vakili-Nezhaad, G., AlNashef, I. M., Asadov, A. & Farid, M. M., Thermogravimetric measurement of deep eutectic solvents vapor pressure. *J. Mol. Liq.* **2016**, 222, 61-66.

(24) Frisch, M. J., Trucks, G. W., Schlegel, H. B., Scuseria, G. E., Robb, M. A., Cheeseman, J. R., Scalmani, G., Barone, V., Mennucci, B., Petersson, G. A., Nakatsuji, H., Caricato, M., Li, X. Y., Hratchian, H. P., Izmaylov, A. F., Bloino, J., Zheng, G., Sonnenberg, J. L., Hada, M., Ehara, M., Toyota, K., Fukuda, R., Hasegawa, J., Ishida, M., Nakajima, T., Honda, Y., Kitao, O., Nakai, H., Vreven, T., Montgomery, J., A., J., Peralta, J. E., Ogliaro, F., Bearpark, M., Heyd, E., Brothers, J. J., Kudin, K. N., Staroverov, V. N., Kobayashi, R., Normand, J., Raghavachari, K., Rendell, A., Burant, J. C., Iyengar, S. S., Tomasi, J., Cossi, M., Rega, N., Millam, J. M., Klene, M., Knox, J. E., Cross, J. B., Bakken, V., Adamo, C., J. Jaramillo, R. Gomperts, R. E. Stratmann, Yazyev, O., Austin, A. J., Cammi, R., Pomelli, C., Ochterski, J. W., Martin, R. L., Morokuma, K., Zakrzewski, V. G., Voth, G. A., Salvador, P., Dannenberg, J. J., Dapprich, S., Daniels, A. D., Farkas, O., Foresman, J. B., Ortiz, J. V., Cioslowski, J. & Fox, D. J., Gaussian, Inc., Wallingford CT. *Gaussian 09, Revision A.02* **2009**.